Hindawi Publishing Corporation
International Journal of Polymer Science
Volume 2016, Article ID 5674572, 8 pages
http://dx.doi.org/10.1155/2016/5674572

Research Article

Effect of Temperature Variation on Bond Characteristics between CFRP and Steel Plate

Shan Li, Tao Zhu, Yiyan Lu, and Xiaojin Li

School of Civil Engineering, Wuhan University, Wuhan 430072, China

Correspondence should be addressed to Yiyan Lu; yylu901@163.com

Received 20 September 2016; Accepted 9 November 2016

Academic Editor: Jun Deng

In recent years, application of carbon fiber reinforced polymer (CFRP) composite materials in the strengthening of existing reinforced concrete structures has gained widespread attention, but the retrofitting of metallic buildings and bridges with CFRP is still in its early stages. In real life, these structures are possibly subjected to dry and hot climate. Therefore, it is necessary to understand the bond behavior between CFRP and steel at different temperatures. To examine the bond between CFRP and steel under hot climate, a total of twenty-one double strap joints divided into 7 groups were tested to failure at constant temperatures from 27°C to 120°C in this paper. The results showed that the joint failure mode changed from debonding along between steel and adhesive interface failure to debonding along between CFRP and adhesive interface failure as the temperature increased beyond the glass transition temperature (T_g) of the adhesive. The load carrying capacity decreased significantly at temperatures approaching or exceeding T_g. The interfacial fracture energy showed a similar degradation trend. Analytical models of the ultimate bearing capacity, interfacial fracture energy, and bond-slip relationship of CFRP-steel interface at elevated temperatures were presented.

1. Introduction

Carbon fiber reinforced polymer (CFRP) has been widely implemented in rehabilitating or strengthening deteriorating structures such as buildings and bridges in civil engineering due to its preferable mechanical properties, including high strength, light weight, corrosion resistance, and formability [1–3]. This has been particularly the case for concrete structures. However, the use of CFRP for strengthening or retrofitting metallic buildings and bridges is still in its early stages [4–6].

In the repair of steel structures with CFRP method, the CFRP is bonded to the steel surface using epoxy adhesives. The load is transferred to the CFRP material by epoxy adhesives. The performance of the CFRP-strengthened steel structures is governed by the effectiveness of interfacial bonding. Therefore, it is necessary to study the bond performance of CFRP-steel interface, through experimental studies on simple CFRP-steel bonded joints. According to it, some researches have been conducted at ambient temperature and revealed that the adhesive layer was the weak link in this composite system, and one of the main failure modes observed was the debonding of CFRP from the steel substrate [7–12].

In some districts where the temperature may exceed 50°C or even higher, mechanical properties of epoxy adhesives may decrease considerably since their T_g are usually in the range from 55 to 120°C [13]. Beyond the T_g value, the adhesive transforms from a glassy state to a rubbery state accompanied with the degradation of the ability to transfer stress efficiently [14–16]. As a result, the mechanical performance of CFRP-strengthened steel structures subjected to elevated temperatures primarily depends on that of the thermoset adhesive. In order to investigate the bond behavior of CFRP-steel systems subjected to elevated-temperature exposure, a few researchers in recent years have undertaken relevant investigations. Nguyen et al. [17] studied the mechanical performance between normal modulus CFRP and steel plate at temperatures around the glass transition temperature (T_g) of the adhesive. A mechanism-based mode to describe the effective bond length, the strength, and the joint stiffness at elevated temperature was presented and verified. Al-Shawaf et al. [18] investigated the bond characteristics of

high modulus CFRP-steel bonded joints using three different epoxy resins at temperatures between 20°C and 60°C. At temperatures near and greater than T_g, as a result of increased adhesive's softening and degradation in properties, the prevailing failure mode was debonding failure, a significant decrease in the ultimate joint load was observed, and the strain level along the CFRP surface almost totally declined. But beyond these, studies on the bond behavior between CFRP and steel at elevated temperatures remain lacking, and further investigation is needed to better understand the performance of CFRP-steel interface at elevated temperatures.

This paper presents results concluded from a series of CFRP-steel double strap joints tested in tension at temperatures ranging from 27°C up to 120°C. Comparisons are presented on failure modes, joint ultimate bearing capacities between specimens at different temperatures. Combining the Chowdhury model [14] and Hart Smith model [19], an analytical model was developed for predicting the ultimate bearing capacity of CFRP-steel joints. Moreover, a model was proposed based on the literature [9, 20, 21] to characterize the temperature dependence of CFRP-steel joint behavior subjected to elevated temperatures.

2. Experimental Program

2.1. Test Specimens. A total of 21 double strap joints divided into 7 groups were tested. Three identical samples were prepared for each specific temperature. For each composite joint, the temperature is the only variable that is changed throughout the experiment (i.e., T = 27, 40, 50, 60, 80, 100, and 120°C). All double strap bond specimens were named in the form of S-Tx. For example, specimen S-T50 strengthened with CFRP composite was tested at 50°C (T50).

2.2. Preparation of Specimens. Figure 1 shows a schematic view of the CFRP-steel double strap joints investigated in this study, including steel substrate, CFRP composite, and adhesive layer. For each specimen, two CFRP sheets were bonded symmetrically to the 3 mm thickness steel surface over a length of 150 mm. In the preparation of the specimen, the surface of the steel plate was uniformly roughened by emery wheel and cleaned with acetone to remove grease, oil, and rust to ensure proper bonding between the composite system and steel. Two CFRP sheets were first cut at 30 mm width and fully infiltrated. After the steel plate was placed in position and the adhesive was applied on the steel surface, the epoxy-bonded CFRP sheets were attached to the desired region and rolled on the adhesive until a uniform bonding layer was formed. All specimens were then cured in the laboratory at ambient temperature for a week.

2.3. Material Properties. Mechanical property of steel plate was obtained through tensile coupon test as per ISO 6892-1 [22]. CFRP sheet was a unidirectional material, and its properties were obtained in accordance with ASTM D3039 [23]. A two-part epoxy adhesive with the glass transition temperature (T_g) being 50°C was applied for all test specimens. The saturant resin (Part A) and hardener (Part B) were mixed

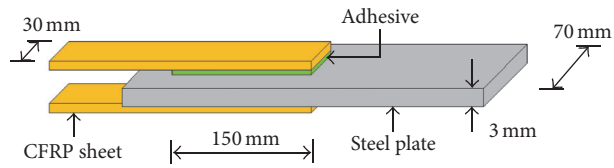

Figure 1: CFRP composite double strap joint specimen.

with a ratio of four to one by weight. Material properties of the two adherends and adhesive are summarized in Table 1.

2.4. Test Setup and Instrumentation. For control specimens, eight strain gauges were attached on the top of the CFRP sheet with spacing of 20 mm in the bonded zone, and one strain gauge in the unbonded zone was used to record the tensile load. For specimens at elevated temperatures, strain measure with adhesively bonded strain gauges is difficult due to the susceptibility of glue and strain gauge to heat. Nevertheless, the displacement values calculated from strain readings basically agree well with the LVDT readings reported by others [10]. Therefore, two L-shaped copper plates, which had a low coefficient of thermal expansion (1.65×10^{-5}/°C), were attached symmetrically for measuring displacement at the loaded end. A device using electric coil for heating was designed for elevated temperature tests. Specimens were preheated in the device to their target temperatures for a period of 20 minutes and kept inside throughout the test process. The arrangements of strain gauges and L-shaped copper plates are shown in Figure 2. All specimens were tested individually in direct tension to failure under displacement control (0.5 mm/min) using a universal hydraulic testing machine (capacity of 100 kN). The schematic view of test setup is shown in Figure 3.

3. Experimental Results

3.1. Failure Mode. Two predominant failure modes could be observed and described as failure Mode I and Mode II. Mode I failure refers to debonding between steel substrate and the adhesive. Mode II failure was debonding between CFRP sheet and the adhesive. The failure modes of all specimens were summarized in Table 2 with selective images of failed specimens presented in Figure 4. Specimens tested at temperatures between 27°C and 50°C were representative of Mode I failure. The debonding initiated from the loaded end and headed to the free end along the steel surface. The results suggest that, at temperatures below T_g, the adhesive used is brittle and glassy and has microcracking propensity, flaws, and imperfections. This will weaken the interfacial adhesive layer and lead to the debonding failure between steel and the adhesive [18]. When heated to tested temperatures from 60 to 120°C, the failure was characteristic of Mode II failure, with a little island-like adhesive left on the steel plate. In addition, more residual epoxy was attached on the surface of the steel plate as the temperature increased. A similar failure mode was observed in previous researches [9, 18, 24]. The epoxy remnant on the steel plate is indicative of poor

Table 1: Material properties.

Material	Thickness (mm)	Young's modulus (GPa)	Yield strength (MPa)	Ultimate strength (MPa)	Failure strain (%)	Shear strength (MPa)
Steel plate	3	205.0	350.0	451.0	20.0	—
CFRP	0.111	252.0	—	3553.0	1.4	—
Epoxy resin[a]	—	2.4		33.0	1.4	21

[a]Manufacturer data.

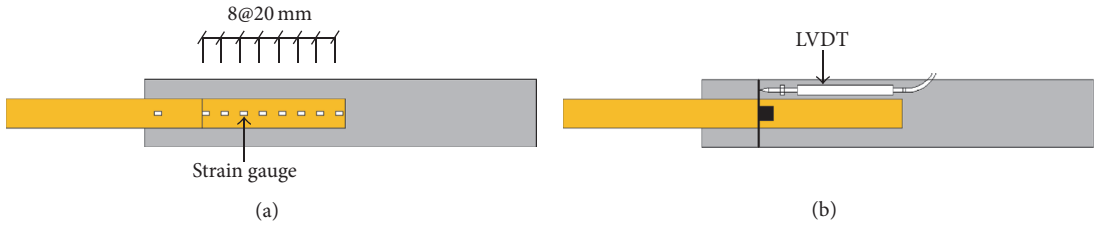

Figure 2: Instrumentation: (a) distribution of strain gauges; (b) layout of LVDTs.

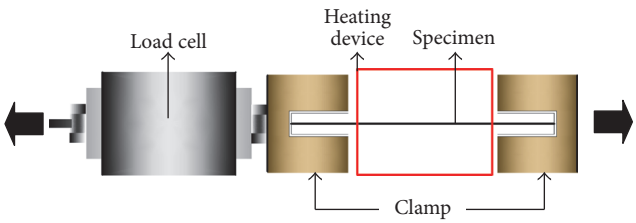

Figure 3: Test setup.

bonding between CFRP sheet and the adhesive. The steel plate and CFRP fibers can maintain their strengths at temperature above 120°C (maximum temperature in this study). This failure shift is believed to be dominated by the temperature dependence of the adhesive layer rather than the adherends. It is also suggested that the adhesive layer may degrade at a faster rate than the resin matrix in CFRP composites. Given that the adhesive and resin matrix were made of the same epoxy polymer, this different ratio in degradation may be because of the composite action between CFRP fibers and resin and different stress levels at adhesive layer and resin matrix [17].

3.2. Load-Displacement Behavior. Figure 5 shows the load-displacement curves for all the specimens. The displacement value for control specimen was calculated from readings of the strain gauges while those for specimens at elevated temperatures were obtained from the LVDT readings. All the curves behaved linearly in the initial loading, followed by a softening stage, and ended with a long plateau until final failure. It is evident from Figure 5 that the initial stiffness of specimens dropped with higher temperature. This degradation was pronounced at temperatures above T_g of the adhesive.

The term "bond strength" refers to the ultimate load that can be resisted by the CFRP sheet before the CFRP sheet debonds from the steel substrate. The bond strengths of all the specimens tabulated in Table 2 are the average values of each series. In the range from 27 to 50°C, the results showed a progressive decrease in bond strength as the temperature increased. The average strengths of S-T40 (10.000 kN) and S-T50 (8.950 kN) are 5.79% and 15.68% lower than that of S-T27 (10.614 kN), respectively. When the temperature exceeded T_g (50°C), a significant reduction of ultimate load was observed. The most drastic drop was seen on specimen S-T120 (0.360 kN), of which the remaining joint bond strength is only 3.39% of the initial strength at 27°C (10.614 kN). This means that there is hardly bond strength between the CFRP sheets and steel plate. This is in line with results reported by others [25]. The internal stress created within the interface due to the volatilization or decomposition as a result of adhesive volume decrease, together with the thermal stress caused by differences of the coefficients of linear thermal expansion of the adhesive and the adherends, would increase the porosity and flaws within the adhesive which, in turn, have a detrimental effect on adhesive-joint capacity.

4. Analysis on Test Results

4.1. Bond Strength Prediction. Based on the failure mode mentioned in Section 3.1, the bond strength of composite joint at ambient temperature can be predicted by the Hart Smith model [19], which was developed based on the adhesive failure of double strap joints. Because $E_s t_s > 2E_f t_f$ in this study, the ultimate load of double strap joint can be written as

$$P_u = \varphi b_f \sqrt{2\tau_a t_a \left(\frac{1}{2}\gamma_e + \gamma_p\right) 4E_f t_f \left(1 + \frac{2E_f t_f}{E_s t_s}\right)} \quad (1)$$

Table 2: Test results of all specimens.

Specimens	Composite	Temperature (°C)	Ultimate load (kN)	Predicted load (kN)	Failure mode
S-T27	CFRP	27	10.614	10.746	I
S-T40	CFRP	40	10.000	10.149	I
S-T50	CFRP	50	8.950	9.309	I
S-T60	CFRP	60	8.056	7.661	II
S-T80	CFRP	80	2.792	3.030	II
S-T100	CFRP	100	1.162	0.901	II
S-T120	CFRP	120	0.360	0.494	II

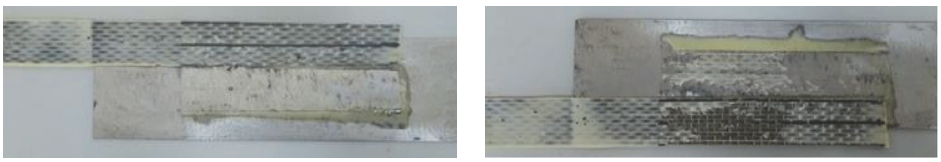

(a) (b)

Figure 4: Typical failure modes: (a) Mode I; (b) Mode II.

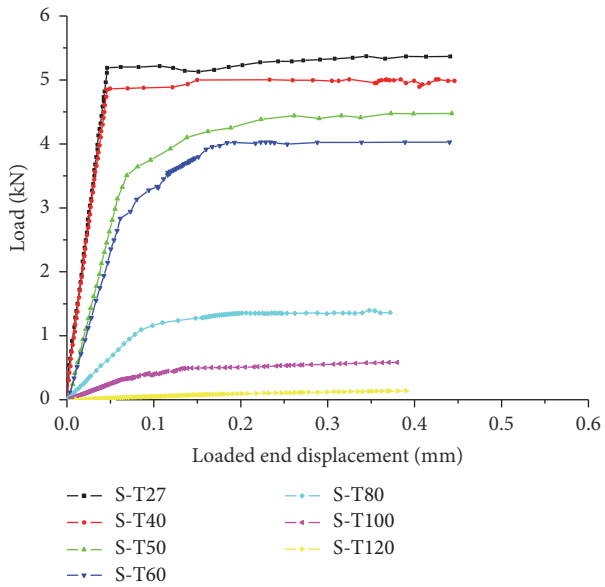

Figure 5: Load-displacement curves.

in which

$$\varphi = \begin{cases} 1 & L \geq L_e \\ \dfrac{L}{L_e} & L < L_e \end{cases}$$

$$L_e = \frac{P_u}{2\tau_a b_f} + \frac{2}{\lambda} \tag{2}$$

$$\lambda = \sqrt{\frac{G_a}{t_a}\left(\frac{1}{E_f t_f} + \frac{2}{E_s t_s}\right)},$$

where φ is the bond length factor; b_f is the width of CFRP composite; τ_a, t_a, γ_e, γ_p, and G_a are the shear strength, thickness, elastic shear strain, plastic shear strain, and shear modulus of adhesive, respectively; E_f, t_f and E_s, t_s are the elastic modulus and thickness of CFRP and steel adherends, respectively; L and L_e are the bond length and effective bond length.

On the other hand, the ultimate loads of specimens at elevated temperatures can be calculated by the Chowdhury model [14], which is given by

$$P_u(T) = \frac{P_u + P_R}{2} - \frac{P_u - P_R}{2}\tanh\left[k\left(T - T'\right)\right], \tag{3}$$

where $P_u(T)$ is the ultimate load of specimen at specific temperature T; P_u is the ultimate load at room temperature obtained by (1); P_R is the residual load capacity; k is a constant; T' is the temperature when a 50% reduction is observed. The values of parameters P_R, k, and T' achieved through regression analysis are equal to 0.422, 0.048, and 68.806, respectively.

All predicted ultimate loads are listed in Table 2. It should be noted that the value of γ_p is taken as $5\gamma_e$ in (1), because this assumption gives much better bond strength prediction in previous research [11]. The good agreement between prediction and test data shown in Figure 6 can be attributed to the fact that the relationship in (3) is totally empirical.

4.2. Discussion on the Interfacial Fracture Energy. The bond strength of a joint well established for CFRP-concrete joint is also applicable to CFRP-steel joint, which is in line with results reported by Xia and Teng [9]. And the double-lap shear test can be treated as two single-lap shear tests being

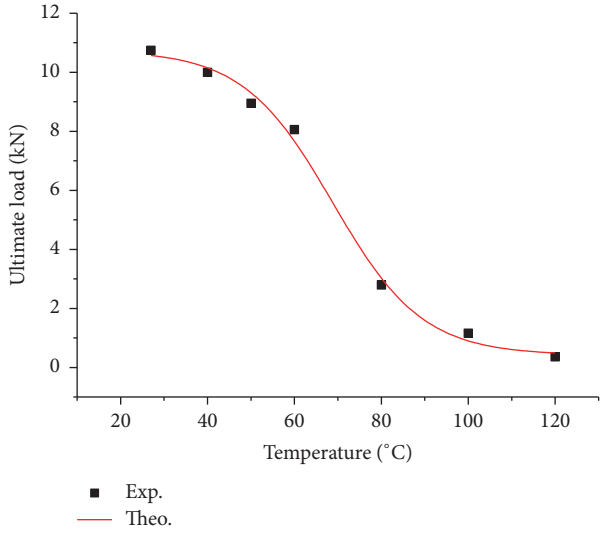

Figure 6: Ultimate load of specimens at elevated temperatures.

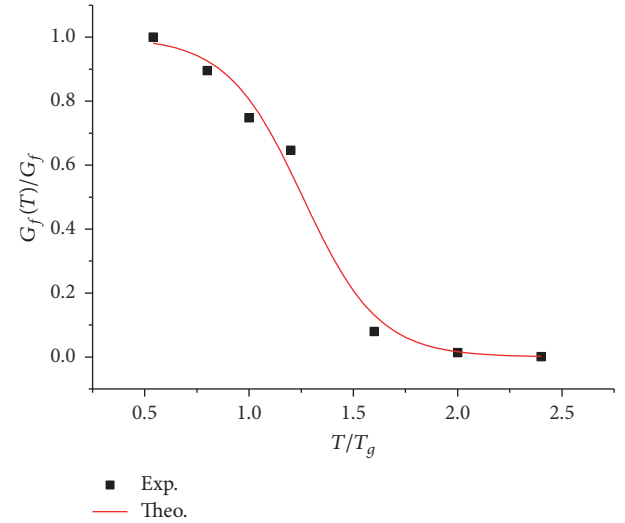

Figure 7: Interfacial fracture energy of specimens at elevated temperatures.

simultaneously conducted, and thus the ultimate load of double strap joint is given by

$$\frac{1}{2}P_u = b_f\sqrt{2G_f E_f t_f}. \tag{4}$$

Taking the effect of thermal exposure into consideration, thus the interfacial fracture energy of specimens at elevated temperatures can be calculated by

$$G_f(T) = \frac{\left[(1/2)\,P_u(T)\right]^2}{2b_f^2 E_f(T)\,t_f}. \tag{5}$$

The effect of elevated temperature is to degrade the mechanical properties of epoxy-impregnated CFRP composite, especially when the temperature exceeds the glass transmission temperature, T_g. According to the degradation model by Bisby [20], the temperature-dependent elastic modulus of CFRP can be calculated by the following equation:

$$\frac{E_f(T)}{E_f} = \frac{1-a_1}{2}\cdot\tanh\left[-a_2\left(T-a_3\right)\right] + \frac{1+a_1}{2}, \tag{6}$$

where $E_f(T)$ is the tensile modulus of CFRP composite at specific temperature T; E_f is the room-temperature modulus; a_1, a_2, and a_3 are the residual values of tensile modulus, constants that describe central temperature and severity of property degradation with temperature, which are 0.869, 0.106, and 52.207, respectively, according to the regression analysis.

Figure 7 depicts how the normalized interfacial fracture energy $(G_f(T)/G_f)$ varies with the normalized temperature (T/T_g). A slight decrease of interfacial fracture energy $G_f(T)$ was observed before T_g approached, whereas a rapid decrease occurred when the temperature exceeds T_g of the adhesive. This decrease is mainly attributed to the mechanical degradation of the adhesive layer. According to the regression analysis, the temperature-dependent interfacial fracture energy can be written as

$$\frac{G_f(T)}{G_f} = \frac{1-b_1}{2}\cdot\tanh\left[-b_2\left(\frac{T}{T_g}-b_3\right)\right] + \frac{1+b_1}{2}, \tag{7}$$

where G_f refers to the interfacial fracture energy at ambient temperature and the regression values of parameters b_1, b_2, and b_3 are 0, 2.762, and 1.257, respectively.

4.3. Shear Stress-Slip Mode. The interfacial shear behavior of adhesively bonded joint is usually characterized by the relationship of the local shear stress and the relative slip between the two adherends. In the double strap joint test, the bond stress between the i-1th strain gauge and the ith strain gauge i, τ_i, can be obtained based on the internal force equilibrium:

$$\tau_i = \frac{E_f t_f\left(\varepsilon_i - \varepsilon_{i-1}\right)}{\Delta x} \quad i \in (2,\ldots,8), \tag{8}$$

where ε_i and ε_{i-1} are measured strains in the CFRP sheet at adjacent strain gauge locations i and $i-1$ which are separated by a distance Δx.

Supposing that there is no relative slip at the free end of CFRP sheet, thus the relative slip s_i, at gauge location i, is expressed as

$$s_i = \frac{\Delta x}{2}\left(\varepsilon_1 + 2\sum_{j=2}^{i-1}\varepsilon_j + \varepsilon_i\right) \quad i \in (2,\ldots,8),\ j \in (2,\ldots,7), \tag{9}$$

where ε_1 is the strain at the free end of CFRP sheet; ε_j is the strain of the jth gauge attached on the CFRP sheet; ε_i is the

strain at the loaded end of CFRP sheet. Using (8) and (9), the local bond-slip relationships along the CFRP-steel interface can be obtained for specimens at ambient temperature.

For specimens at elevated temperatures without strain gauges, the bond-slip curve can be obtained from the relationship between the CFRP strain and slip at the loaded end. According to the literature [9, 10, 12, 21, 26–28], the bond-slip curves for CFRP-steel bonded joints are similar to those for CFRP-concrete bonded joints; both have a bilinear shape. And their developments of shear stress are the same. At a low load, the interface is in an elastic stage, during which the shear stress is the largest at or very close to the loaded end and gradually decreases towards the free end. As the load increases, part of the interface enters into softening stage, during which the shear stress at the loaded end decreases after it has approached its maximum value. When the shear stress at the loaded end reduces to zero, the ultimate load of the specimen is reached and keeps almost constant; debonding commences and propagates along the interface towards the free end with the peak shear stress moving gradually towards the free end. On the other hand, the strain-slip curves at the loaded end in this study derived from the load-slip relationship for CFRP-steel bonded joints are similar to those for CFRP-concrete bonded joints. Therefore, a similar expression linked to an exponential term is proposed for the relationship of the CFRP strain and interfacial slip in this section based on existing analytical model [21]:

$$\varepsilon = f(s) = \alpha\left(1 - e^{-\beta s}\right), \tag{10}$$

where α and β are regression parameters.

Figure 8 shows the comparison between regressing curves and experimentally observed relationships. It is found that all the ε-s curves predicted for specimens at elevated temperatures match well the experimental relationships plotted.

On the other hand, the equation of forces equilibrium acting on the CFRP sheet can be written as

$$\frac{d\sigma_f}{dx} - \frac{\tau}{t_f} = 0, \tag{11}$$

where σ_f and τ are the axial stress in the CFRP sheet and shear stress in the adhesive layer at any location, respectively. Combining (10) and (11) and neglecting the strain of the steel plate yield the following equation for the τ-s curve:

$$\begin{aligned}\tau &= t_f \frac{d\sigma_f}{dx} = E_f(T)\, t_f \frac{d\varepsilon}{dx} = E_f(T)\, t_f f(s) \frac{df(s)}{ds} \\ &= \alpha^2 \beta E_f(T)\, t_f e^{-\beta s}\left(1 - e^{-\beta s}\right)\end{aligned} \tag{12}$$

because

$$G_f(T) = \int_0^\infty \tau ds = \frac{1}{2}\alpha^2 E_f(T)\, t_f. \tag{13}$$

The τ-s relationship can be rewritten as

$$\tau = 2G_f(T)\, \beta e^{-\beta s}\left(1 - e^{-\beta s}\right). \tag{14}$$

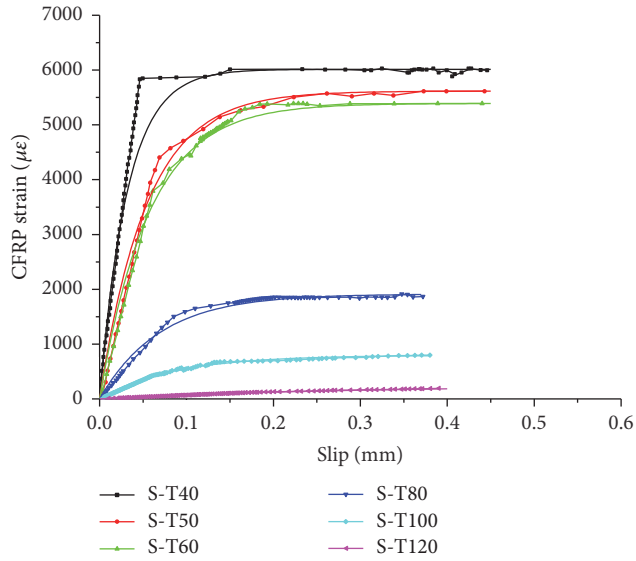

Figure 8: Relationships of CFRP strain and slip at loaded end.

Therefore, the shear stress as a function of relative slip can be determined with $G_f(T)$ calculated by (7) and regression parameter β.

Figure 9 shows how the normalized maximum shear stress ($\tau_{max}(T)/\tau_{max}$) and the corresponding normalized slip ($s_{max}(T)/s_{max}$) vary with the normalized temperature (T/T_g). The effect of elevated temperature is easier to characterize, showing typically a decrement of maximum shear stress with larger corresponding relative interfacial slip. The maximum bond stress decreased in agreement with the lower interfacial fracture energy, while the increase in slip meant degradation in the interfacial stiffness because of the softening of the adhesive.

5. Conclusions

The experimental results of 21 double strap joints subjected to elevated temperatures are presented. It is found that the CFRP-steel interface is significantly weakened and the degradation is affected by thermal exposure. The following conclusions are reached within the scope of this research:

(1) The failure mode of specimens was affected by the elevated-temperature exposure. It was likely to change from debonding along steel-adhesive failure to debonding along CFRP-adhesive failure. The change of failure mode is dominated by the degradation and volume decrease of the adhesive.

(2) The thermal exposure tended to decrease the initial stiffness and ultimate load for specimens, especially at temperatures above T_g of the adhesive.

(3) A model was developed based on the Hart Smith model and the Chowdhury model for predicting the ultimate bearing capacity.

(4) The interfacial fracture energy decreased gently at temperature below T_g, but much sharply when the

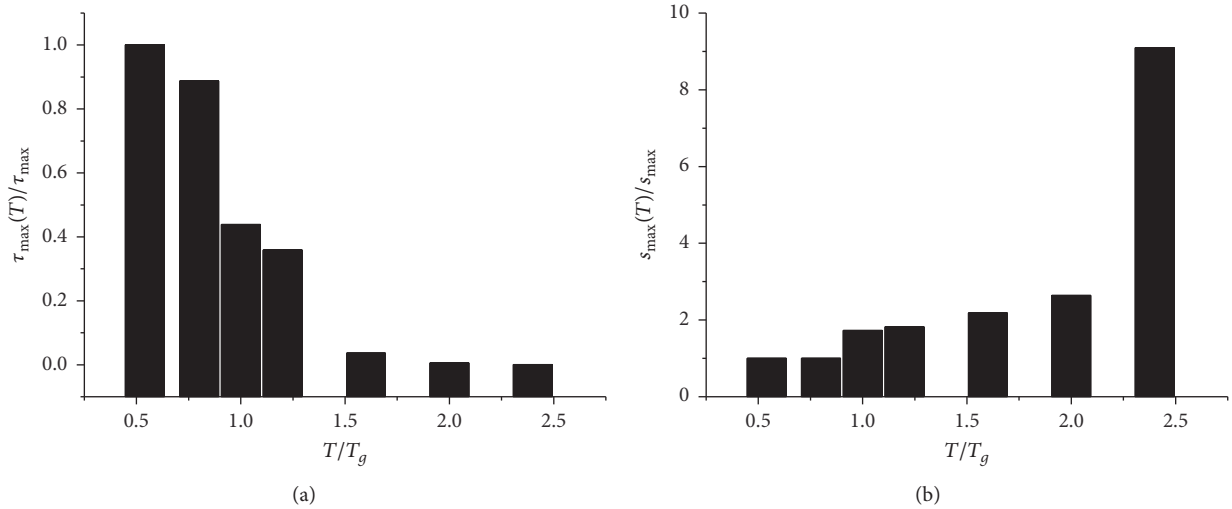

Figure 9: Effect of elevated temperatures on (a) τ_{max} and (b) s_{max}.

temperature exceeded T_g. A degradation model of interfacial fracture energy was presented.

(5) Bond-slip relationship that approximates the effect of thermal exposure through regression parameters, calibrated by experimental data, was suggested. CFRP-steel interfaces at elevated temperatures showed a decrement of the maximum bond stress attained at a larger slip.

Competing Interests

The authors declare no competing interests.

Acknowledgments

The tests reported herein were made possible by the financial support from the Natural Science Foundation of China (51578428). The authors wish to thank the civil engineering technicians of Wuhan University for their help throughout the test process.

References

[1] L. C. Hollaway, "A review of the present and future utilisation of FRP composites in the civil infrastructure with reference to their important in-service properties," *Construction and Building Materials*, vol. 24, no. 12, pp. 2419–2445, 2010.

[2] J.-G. Dai, Y.-L. Bai, and J. G. Teng, "Behavior and modeling of concrete confined with FRP composites of large deformability," *Journal of Composites for Construction*, vol. 15, no. 6, pp. 963–973, 2011.

[3] Y. Y. Lu, N. Li, and S. Li, "Behavior of FRP-confined concrete-filled steel tube columns," *Polymers*, vol. 6, no. 5, pp. 1333–1349, 2014.

[4] D. Schnerch and S. Rizkalla, "Flexural strengthening of steel bridges with high modulus CFRP strips," *Journal of Bridge Engineering*, vol. 13, no. 2, pp. 192–201, 2008.

[5] A. H. Al-Saidy, F. W. Klaiber, and T. J. Wipf, "Strengthening of steel-concrete composite girders using carbon fiber reinforced polymer plates," *Construction and Building Materials*, vol. 21, no. 2, pp. 295–302, 2007.

[6] J. G. Teng, T. Yu, and D. Fernando, "Strengthening of steel structures with fiber-reinforced polymer composites," *Journal of Constructional Steel Research*, vol. 78, no. 6, pp. 131–143, 2012.

[7] R. Haghani, "Analysis of adhesive joints used to bond FRP laminates to steel members—a numerical and experimental study," *Construction and Building Materials*, vol. 24, no. 11, pp. 2243–2251, 2010.

[8] S. Fawzia, R. Al-Mahaidi, and X.-L. Zhao, "Experimental and finite element analysis of a double strap joint between steel plates and normal modulus CFRP," *Composite Structures*, vol. 75, no. 1–4, pp. 156–162, 2006.

[9] S. H. Xia and J. G. Teng, "Behaviour of FRP-to-steel bonded joints," in *Proceedings of the International Symposium on Bond Behaviour of FRP in Structures (BBFS '05)*, pp. 411–418, Hong Kong, December 2005.

[10] T. Yu, D. Fernando, J. G. Teng, and X. L. Zhao, "Experimental study on CFRP-to-steel bonded interfaces," *Composites Part B: Engineering*, vol. 43, no. 5, pp. 2279–2289, 2012.

[11] C. Wu, X. L. Zhao, W. H. Duan, and R. Al-Mahaidi, "Bond characteristics between ultra high modulus CFRP laminates and steel," *Thin-Walled Structures*, vol. 51, no. 2, pp. 147–157, 2012.

[12] S. Fawzia, X.-L. Zhao, and R. Al-Mahaidi, "Bond-slip models for double strap joints strengthened by CFRP," *Composite Structures*, vol. 92, no. 9, pp. 2137–2145, 2010.

[13] D. Cree, T. Gamaniouk, M. L. Loong, and M. F. Green, "Tensile and lap-splice shear strength properties of CFRP composites at high temperatures," *Journal of Composites for Construction*, vol. 19, no. 2, Article ID 04014043, 2015.

[14] E. U. Chowdhury, R. Eedson, L. A. Bisby, M. F. Green, and N. Benichou, "Mechanical characterization of fibre reinforced polymers materials at high temperature," *Fire Technology*, vol. 47, no. 4, pp. 1063–1080, 2011.

[15] A. P. Mouritz and A. G. Gibson, *Fire Properties of Polymer Composite Materials*, Springer, Dordrecht, The Netherlands, 2006.

[16] S. Cao, Z. Wu, and X. Wang, "Tensile properties of CFRP and hybrid FRP composites at elevated temperatures," *Journal of Composite Materials*, vol. 43, no. 4, pp. 315–330, 2009.

[17] T.-C. Nguyen, Y. Bai, X.-L. Zhao, and R. Al-Mahaidi, "Mechanical characterization of steel/CFRP double strap joints at elevated temperatures," *Composite Structures*, vol. 93, no. 6, pp. 1604–1612, 2011.

[18] A. Al-Shawaf, R. Al-Mahaidi, and X.-L. Zhao, "Effect of elevated temperature on bond behaviour of high modulus CFRP/steel double-strap joints," *Australian Journal of Structural Engineering*, vol. 10, no. 1, pp. 63–74, 2009.

[19] L. J. Hart Smith, "Adhesive-bonded double-lap joints," Tech. Rep. NASA CR-112235, Douglas Aircraft Company, Long Beach, Calif, USA, 1973.

[20] L. Bisby, *Fire behavior of fiber-reinforced polymers (FRP) reinforced or confined concrete [Ph.D. thesis]*, Queens University, Ontario, Canada, 2003.

[21] J.-G. Dai, W. Y. Gao, and J. G. Teng, "Bond-slip model for FRP laminates externally bonded to concrete at elevated temperature," *Journal of Composites for Construction*, vol. 17, no. 2, pp. 217–228, 2013.

[22] ISO, "Metallic materials-tensile testing-part 1: method of test at room temperature," ISO 6892-1:2009, BSI, London, UK, 2009.

[23] *Standard Test Method for Tensile Properties of Polymer Matrix Composite Materials; ASTM D3039-07*, ASTM, West Conshohocken, Pa, USA, 2008.

[24] R. Haghani and M. Al-Emrani, "A new design model for adhesive joints used to bond FRP laminates to steel beams part B: experimental verification," *Construction and Building Materials*, vol. 30, no. 5, pp. 686–694, 2012.

[25] Y. Y. Lu, W. J. Li, S. Li, X. Li, and T. Zhu, "Study of the tensile properties of CFRP strengthened steel plates," *Polymers*, vol. 7, no. 12, pp. 2595–2610, 2015.

[26] H. Yuan, J. G. Teng, R. Seracino, Z. S. Wu, and J. Yao, "Full-range behavior of FRP-to-concrete bonded joints," *Engineering Structures*, vol. 26, no. 5, pp. 553–565, 2004.

[27] J. G. Dai, T. Ueda, and Y. Sato, "Development of the nonlinear bond stress-slip model of fiber reinforced plastics sheet-concrete interfaces with a simple method," *Journal of Composites for Construction*, vol. 9, no. 1, pp. 52–62, 2005.

[28] J. G. Dai, T. Ueda, and Y. Sato, "Unified analytical approaches for determining shear bond characteristics of FRP-concrete interfaces through pullout tests," *Journal of Advanced Concrete Technology*, vol. 4, no. 1, pp. 133–145, 2006.